

# Diversity of rhizospheric fungi from *Nanhaia speciosa* and their capacity to degrade insoluble phosphate and organic matters

PHONG XUAN ONG<sup>1</sup>, THIEP VAN NGUYEN<sup>1</sup>, LIEN THUY BUI<sup>1</sup>, NGUYEN THI MINH NGUYET<sup>1</sup>, KHANG TAN DO<sup>2</sup>, GIA HUY TRAN<sup>2</sup>, PHI BANG CAO<sup>3</sup>, HA DUC CHU<sup>4</sup>, NGOC BICH PHAM<sup>5</sup>, THACH VAN PHAN<sup>6</sup>, HONG VIET LA<sup>1,✉</sup>

<sup>1</sup>Institute for Scientific Research and Application, Hanoi Pedagogical University 2, Nguyen Van Linh Street, Xuan Hoa Ward, Phuc Yen City, Vinh Phuc Province 280000, Vietnam. Tel.: +84-211-3512468, ✉email: laviethong@hpu2.edu.vn

<sup>2</sup>Institute of Food and Biotechnology, Can Tho University, Xuan Khanh, Ninh Kieu, Can Tho City 900000, Vietnam

<sup>3</sup>Faculty of Natural Science, Hung Vuong University, Nong Trang Ward, Viet Tri City 35000, Phu Tho Province, Vietnam

<sup>4</sup>Faculty of Agricultural Technology, University of Engineering and Technology, Vietnam National University Hanoi, Xuan Thuy Street, Cau Giay District, Hanoi City 122300, Vietnam

<sup>5</sup>Institute of Biotechnology, Vietnam Academy of Science and Technology, Hoang Quoc Viet Road, Cau Giay District, Hanoi City 122300, Vietnam

<sup>6</sup>Department of Biotechnology, NTT Hi-tech Institute, Nguyen Tat Thanh University, 300A Nguyen Tat Thanh Street, Ward 13, District 4, Ho Chi Minh City, Vietnam

Manuscript received: 27 July 2024. Revision accepted: 12 October 2024.

**Abstract.** Ong PX, Nguyen TV, Bui LT, Nguyet NTM, Do KT, Tran GH, Cao PB, Chu HD, Pham NB, Phan TV, La HV. 2024. Diversity of rhizospheric fungi from *Nanhaia speciosa* and their capacity to degrade insoluble phosphate and organic matters. *Biodiversitas* 25: 3585-3595. The rhizosphere is the microenvironment for interactions between plant roots and surrounding microbes. Rhizospheric fungi play a vital role in plant growth through various mechanisms. The aim of this study was to isolate and identify the fungi from the soil around the root of *Nanhaia speciosa* (Champ. ex Benth.) J.Compton and Schrire and to test their ability to degrade insoluble phosphate, cellulose, and xylan. The result showed that a total 72 fungal species were isolated from the soil of the rhizosphere of *N. speciosa*. These isolates belonged to six genera, namely *Penicillium*, *Trichoderma*, *Aspergillus*, *Talaromyces*, *Purpureocillium*, and *Chaetomium*. Results showed that 50% of the isolated strains belonged to the genus *Penicillium*. Moreover, it was also recorded that out of 10 fungal strains, only five fungal strains produced the phosphate decomposition enzyme (+), with the Tv-LHOP3 (*Trichoderma virens* LHOP3) and Tk-LHOP1 (*Trichoderma koningiopsis* LHOP1) strains expressed the highest phosphate solubility with the PSI of two strains were 2.22 and 2.18, respectively. All strains exhibited cellulose ability, Pj-LHOP2 (*Penicillium janthinellum* LHOP2) showed the highest degradation ability with a halo diameter of 7.52 cm, followed by strain Tk-LVHOP1 (*Trichoderma koningiopsis* LHOP1) with a diameter of 7.38 cm. The xylan degradation ability test demonstrated that the strain Tv-LHOP2 (*Trichoderma virens* LHOP2) had the highest halo diameter of 8.87 cm, followed by Tk-LHOP1 (*Trichoderma koningiopsis* LHOP1) had 8.80 cm and Tv-LHOP3 (*Trichoderma virens* LHOP3) had halo diameter of 8.63 cm. These findings suggest the potential of these fungal strains as biofertilizers to enhance nutrient availability and promote sustainable agricultural practices, particularly in improving the growth and yield of medicinal plants like *Nanhaia speciosa*.

**Keywords:** Diversity, insoluble phosphate, *Penicillium* sp., *Nanhaia speciosa*, rhizospheric fungi, xylan

**Abbreviations:** Pj-LHOP2: *Penicillium janthinellum*; Ps-LHOP1: *Penicillium simplicissimum*; Tp-LHOP1: *Talaromyces pinophilus*; Tv-LHOP1: *Trichoderma virens*; Ac-LHOP1: *Aspergillus carbonarius*; Tv-LHOP2: *Trichoderma virens*; Pl-LHOP1: *Purpureocillium lilacinum*; Tk-LHOP1: *Trichoderma koningiopsis*; Tv-LHOP3: *Trichoderma virens*; Cc-LHOP1: *Chaetomium cuperum*

## INTRODUCTION

The rhizosphere is a microenvironment around 0 to 2 mm between the soil and the root surface that serves as the site of energy exchange between the plant and the soil. Most plants naturally have a symbiotic relationship with rhizospheric fungi, which give them nitrogen and phosphorus (P) in exchange for the use of their roots. This advantageous association can greatly increase the efficiency with which plants use the nutrients found in the soil (Rilling et al. 2019), specifically in the rhizosphere of *Drepanostachyum luodianense* (T.P.Yi & R.S.Wang) Keng f., a fungal diversity test identified 33 isolates as belonging to 24 species of 12 genera, with *Penicillium* being the

dominant genus (Liu et al. 2017).

Most fungal strains have been used as microbial fertilizers for promoting the solubility of insoluble phosphate and the decomposition of organic matter (cellulose and xylan, a main component of hemicellulose), supporting sustainable agriculture (Bhattacharyya et al. 2020; Bala 2022). Phosphate-solubilizing fungi can generate organic acids, mobilize and improve nutrient uptake, and increase the effectiveness of phosphate fertilizers such as rock phosphate and superphosphate. Several fungal strains were isolated from Moso bamboo rhizosphere soil, among which *Aspergillus neoniger* and *Talaromyces aurantiacus* were able to thrive in acidic environments and also had the remarkable ability to release soluble P through the

breakdown of resistant P-containing compounds (Zhang et al. 2018). 30 rock phosphate solubilizing fungi as biofertilizers have been evaluated for their ability to solubilize rock phosphate, of which three fungi demonstrated significant solubilization, with potential benefits for plant growth (Sane and Mehta 2015).

Cellulose has a macromolecular complex that makes up the majority of unused agricultural biomass. Four superior strains were selected for cellulose degradation, including *Cladosporium cladosporioides*, *Aspergillus sydowi*, *Penicillium waksmanii*, and *Plectosphaerella* sp. (Han et al. 2008). M'barek et al. (2019) isolated and screened several high-performing lignocellulolytic fungi, including *Mucor circinelloides*, *Mucor racemosus*, *Penicillium brasilianum*, *Penicillium crustosum*, *Paecilomyces* sp., *Fusarium oxysporum*, *Fusarium solani*, *Aspergillus fischeri*, *Curvularia spicifera*, *Humicola grisea*, *Trichoderma atroviride*, and *Cosmospora viridescens*, from decaying plant material (M'barek et al. 2019). Elfiati et al. (2019) identified cellulolytic fungi from local Raru species in Indonesia, of which *Aspergillus terreus* is the most abundant. Several ligninolytic fungi from soil samples in Egypt, including *G. lucidum*, *L. edodes*, and *T. harzianum*, were isolated and identified (Bedaiwy et al. 2022). Furthermore, the first identification of the lignivorous fungus was *Paecilomyces maximus* in decayed cedar wood in Morocco (Chauiyakh et al. 2023).

Xylan is the second most abundant renewable polysaccharide on Earth, and its degradation provides nutrients for plants. However, it is difficult to break down. *Trichoderma*, *Aspergillus*, and *Penicillium* are known for producing xylanase enzyme to decompose xylan (Bhardwaj et al. 2019; Méndez-Líter et al. 2021). These studies collectively highlight the rich and varied fungal communities in the rhizosphere of medicinal plants, with potential implications for plant health and biocontrol.

*Nanhaia speciosa* (Champ. ex Benth.) J.Compton and Schrire is an important medicinal plant of the Fabaceae well known for its ability to effectively treat chronic bronchitis, arthritis, cough, numbness in the wrists or knees, low blood flow, anemia, tuberculosis, and chronic hepatitis (Huang et al. 2020; Yao et al. 2021). As *N. speciosa* contains a large number of bioactive components, including saponins, flavonoids, phenolic glycosides, polysaccharides, and formononetin, it is used in traditional medicine (Yu and Liang 2019; Huang et al. 2020). The beneficial microbial populations found in the rhizosphere are usually referred to as plant growth-promoting microorganisms. However, research on microbial communities, especially fungal communities in the rhizosphere of *N. speciosa*, still needs to be improved. The aim of this study was to assess the abundance of the fungal community in the rhizosphere of *N. speciosa* and to test their ability to degrade phosphate, cellulose, and xylan.

## MATERIALS AND METHODS

### Rhizospheric soil sample collection

Soil samples around the roots of *N. speciosa* were

collected from Lang Son, Bac Giang, and Vinh Phuc provinces, Vietnam. Rhizospheric soil samples from a depth of 10 to 25 cm from the surface were collected in sterilized, clean, dry polythene bags. The soil samples were taken to the laboratory and stored at 4°C in the refrigerator for further analysis.

### Isolation and selection of microorganisms

Isolation involved dilution method, wherein 1 g of the soil sample was suspended in a test tube with 10 mL of sterilized distilled water and shaken on a vortex to dissolve evenly. The sample solution was continuously diluted to 10<sup>-5</sup> concentrations. 0.5 mL of the desired concentration was inoculated on Petri dishes containing PDA (Potato Dextrose Agar) medium. A triangular glass stick was used to spread evenly on the surface and incubated at room temperature (Nafaa et al. 2023). Once the fungus grew on PDA medium, it was purified using the single-spore culture method.

### Morphological identification of fungal isolates

The fungal isolates were identified on the basis of morphological characteristics, such as color and texture of colony, while microscopic characteristics, included shape of conidia, conidiophores, and spore arrangement. Additionally, lactophenol cotton blue was used for slide preparation, and images were viewed under a microscope (Primostar, Carl Zeiss) with 10× and 40× objectives for microphotographs.

### Molecular identification

#### DNA extraction

Pure cultures of fungal colonies were used for DNA extraction, following the procedure of Roger and Bendich (1989) with appropriate modifications (Rogers and Bendich 1989). The genomic DNA quantity and quality were evaluated using a Nanodrop spectrophotometer.

#### Amplification of ITS region

For molecular identification, the nuclear DNA barcode, internal transcribed spacer (ITS) region was amplified with the primer pair ITS1 (5'-TCCGTAGGTGAACCTGCGG-3') and ITS4 (5'-TCCTCCGCTTATTGATATGC-3') (White et al. 1990). The reaction was conducted in a 30 µL volume, including 15 µL of Mytaq mix (Bioline, England), 0.5 µL of each primer (forward and reverse, each of 20 µM), and 2 µL DNA template (50 ng.µL<sup>-1</sup>). The thermal cycle was as follows: initial denaturation for 5 min at 95°C, followed by 35 cycles of denaturation for 1 minute at 94°C, annealing for 30 seconds at 57°C, extension for 90 seconds at 72°C and a final extension step at 72°C for 10 minutes. Subsequently, all PCR products were visualized using gel electrophoresis in 2% agarose. The specific amplicons of the purified fragments were then directly subjected to Sanger sequencing (DNA Sequencing Inc., Vietnam). In this study, the ITS region of 10 isolates was sequenced to support identifying the fungal isolates.

#### Sequence analysis and phylogenetic construction

From the chromatogram files, raw sequences were interpreted by Bioedit software version 7.2.1. After

unidentified signals were trimmed, sequences were saved in FASTA format for further analysis. Sequences were submitted to the nucleotide BLAST (Basic Local Alignment Search Tool) and compared to the database of ITS region from fungi and type materials for identification. The data set involved 26 sequences from this study, and the reference sequences were collected from the NCBI database based on pairwise identity. Multiple sequence alignment was performed following the ClustalW algorithm, and the conservative and variable sites were determined. The phylogenetic tree was inferred by the Kimura 2-parameter model Maximum Likelihood method and 1000 bootstrap replicas. Trees were drawn to scale by the number of substitutions per site with branch lengths measured. There was a total of 477 positions in the final dataset. All analyses were conducted in MEGA11 (Tamura et al. 2021).

### Characterization of the decomposition ability for insoluble phosphate, cellulosic cellulose, and xylan

#### Phosphate solubilizing test

The ability of each of fungal strains to solubilize phosphate was tested using Pikovskaya's agar plate (PVK) with added 5% tricalcium phosphate; this compound served as a source of insoluble phosphate. Fungal colonies were recorded after 1, 3, and 5 days of culture at 25°C (Wakelin et al. 2007; Doilom et al. 2020). The clear halo zone surrounding the fungal colony after incubation was measured to determine the insolubilized phosphate-degrading ability of isolates following formulas: The P Solubilization Index (PSI) is calculated as  $(C+Z)/C$ , where C and Z are colony and halo zone diameters, respectively.

#### Cellulose decomposition test

Ten selected fungal isolates were cultured in Peptone Yeast Glucose (PYG) agar plate. When the fungus grew to about 50% of the Petri dish, it was transferred to a cellulolysis basal medium (CBM) agar plate with 2% carboxymethyl cellulose (CMC). Colonies grew to plates, on which Congo Red reagent (2%) was applied for 15 min. Then, Congo reagent was discarded and washed with distilled water. After being washed, the plates were soaked in a NaCl solution (the ratio of NaCl to water was 1:1); and the clarity of medium was checked (opaque yellow was used as a sign of decomposed cellulose; red background was undecomposed CMC). To calculate the cellulolytic

activity, diameter of clear zones surrounding the fungal colonies, indicating cellulose degradation, was measured after 15 to 24 hours (Tolan and Foody 1999).

#### Xylan decomposition test

The xylan degradation of fungal isolates was assessed by their xylanase production ability using a xylanolysis basal medium (XBM) of 1.6% (w/v) agar supplemented with 0.4% (w/v) glucose. To selectively induce xylanase production, isolates were subcultured in a medium supplemented with 0.5% beach wood xylan as a carbon source. After incubation at 30°C for 5 days, 1% iodine reagent solution was applied to the surface plate. After 15 minutes, iodine was discarded, and plates were rinsed with distilled water. The color change of the mycelium around colonies was observed, and the diameter of the cleaning circle was measured to evaluate the xylanolytic activity of isolates from 15 minutes to 24 hours (Pointing 1999).

#### Statistical analysis

All experiments were performed with three replications in a completely randomized design. Measured data (P solubilization index, enzyme assay) from different treatments were calculated and statistically analyzed by Statistical Package for the Social Sciences (SPSS) for Windows version 22 (SPSS, Inc., Chicago, IL, United States). Significant differences were evaluated using Duncan's multiple range test between mean values at  $p < 0.05$ .

## RESULTS AND DISCUSSION

### Diversity and morphological description of fungal isolates

The present study was focused on the isolation and identification of fungal strains from the rhizosphere of cultivated *N. speciosa* from Vinh Phuc, Bac Giang, and Lang Son provinces. A total of 72 fungal isolates were obtained, of which 30 were from Bac Giang, 10 from Lang Son, and 32 from Vinh Phuc. Most of the fungal isolates were morphologically identified at the genus level as *Penicillium*, *Trichoderma*, *Aspergillus*, *Talaromyces*, *Purpureocillium*, and *Chaetomium*. The relative abundance of each fungal isolate and taxa showed difference between sampling locations (Figure 1).

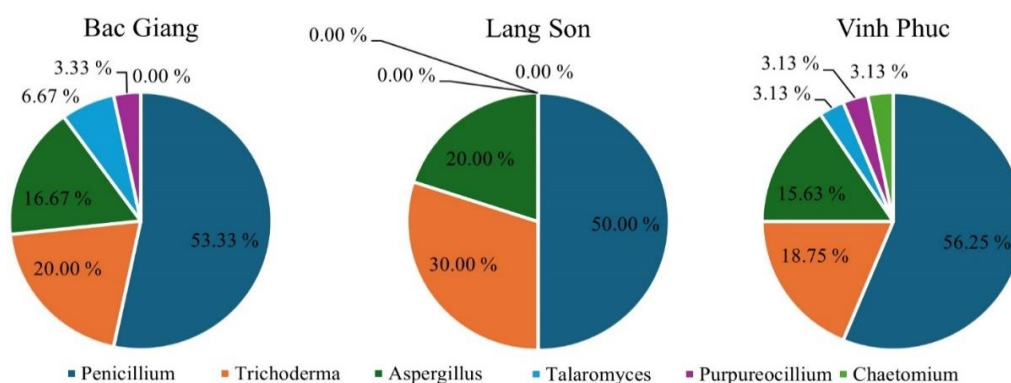


**Figure 1.** The relative abundance (%) of fungal isolates from the different sampling locations

In specific terms, Vinh Phuc had the highest abundance of fungal genera, with members of six genera, followed by Bac Giang which had five genera and the lowest relative abundance was recorded from Lang Son, which had three genera. It is noteworthy that in all three research locations, the majority (>50%) of the strains were from the genus *Penicillium*. A similar fungal diversity (12 species of *Penicillium*) was observed in the rhizosphere soil of *D. luodianense* (Liu et al. 2017). The soil fungal community composition and abundance varied between seasons, and the richness of microbial community is negatively correlated with temperature and precipitation (Zhao et al. 2023). Moreover, increasing forest age led to more specific bacterial and fungal associations (Li et al. 2022). In this study, the abundance of fungal genera in the rhizosphere of *N. speciosa* could be affected by the soil compositions between the collected sampling locations. Ten representative strains of 6 fungal genera were morphologically identified, and their characterizations are shown in Table 1.

### Molecular identification based on the ITS gene region

#### Sequence characteristics

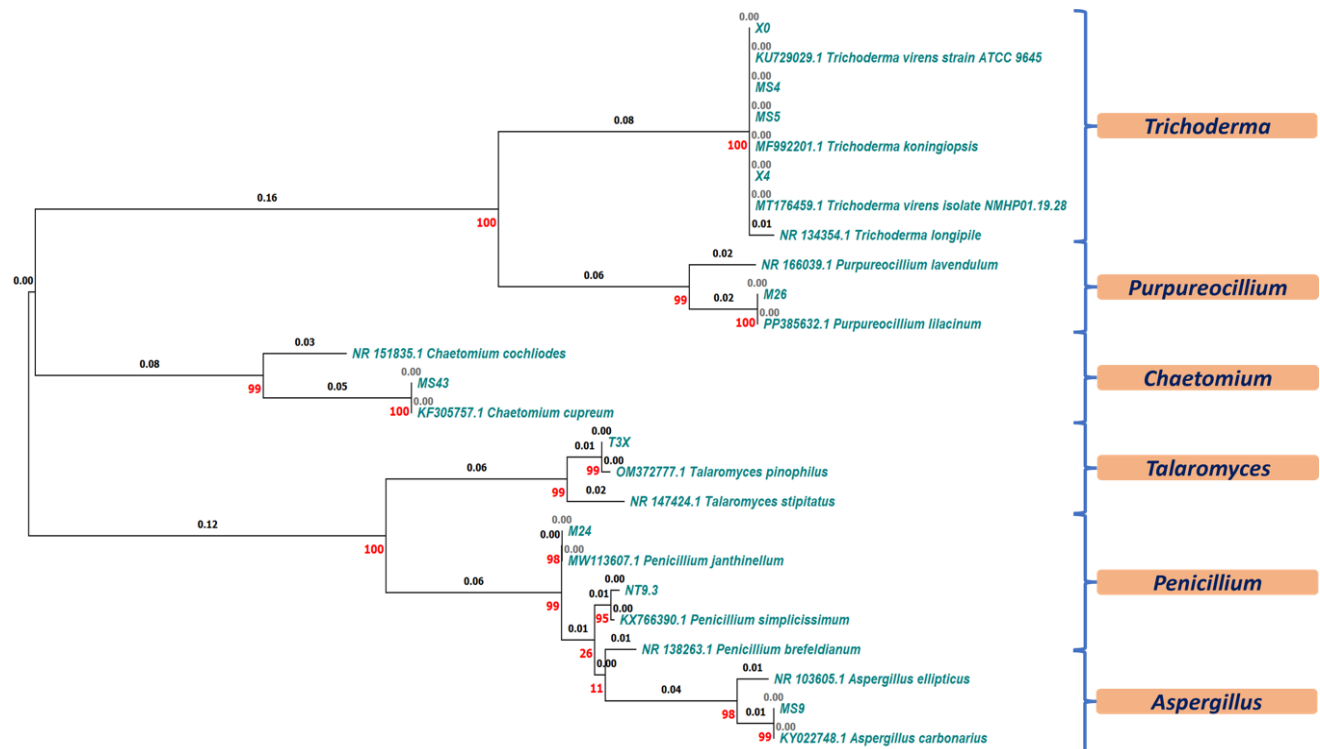
After removing two ends, the 10 ITS sequences ranged in length from 446 to 529 bp. The strong signal from the chromatogram confirmed the sequence quality. Based on the percentage of identity against the NCBI database, 10 fungal strains were classified into six genera, including *Penicillium*, *Talaromyces*, *Aspergillus*, *Trichoderma*,

*Purpureocillium*, and *Chaetomium*. The scientific names of 10 isolates are given in Table 2.

#### Phylogenetic tree

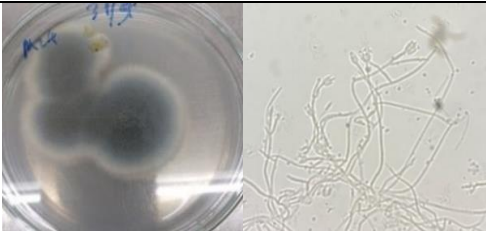
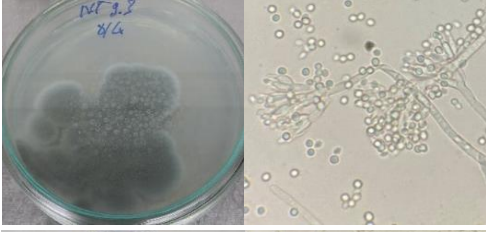
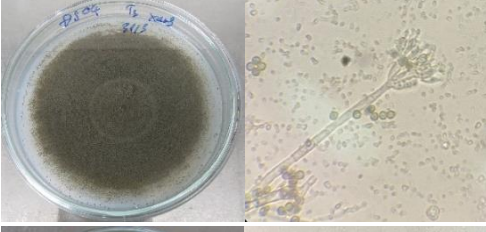
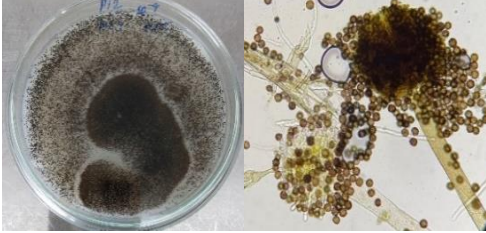
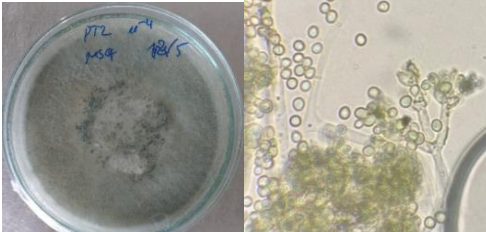
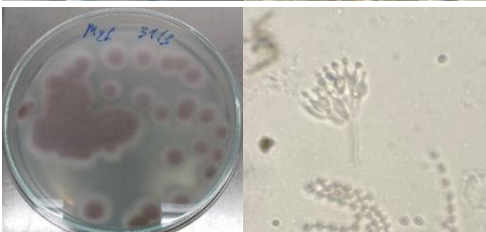
The ITS region of the internal transcribed spacer was sequenced with utmost care and precision to identify the fungal isolates according to phylogenetics (Figure 2). The phylogenetic analysis involved 26 nucleotide sequences from both this study and the NCBI database. After ignoring the ambiguously aligned regions, the aligned lengths were 477 bp and 228 bp, which were phylogenetically informative. Eight species were identified by phylogeny and supported by the BLAST results. The branch length reflected the genetic distance between the query sequence (this study) and the NCBI reference sequence. Therefore, the shorter branch length indicated the more identical level among them, while other species were located in the separated branch.

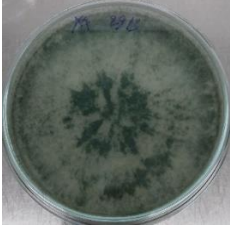
The high bootstrap value was 99-100%, so the reliability of the phylogeny model was confirmed. However, in the case of the 4 strains, including MS5, MS4, X4, and X0, the ITS sequence showed a weak level of species discrimination. These 4 strains and 2 species, *Trichoderma virens* and *Trichoderma koningiopsis* were classified into a monophyletic group. Due to this limitation, additional DNA barcodes should be combined for further studies (Raja et al. 2017).



**Figure 2.** The phylogeny tree of 10 selected isolates and closely related species was recovered from GenBank based on ITS sequences. The expressed value on each branch was the Bootstrap of 1000 replications

**Table 1.** Morphological characterization of the fungal isolates on PDA medium

Isolates	Macroscopic colony and microscopic characterization	Morphological identification and description
M24		<p><i>Penicillium</i> sp. 1: Circular colonies were spongy and grey-green in color. The edge of colony was white. Fungal hyphae were colorless and septate. Conidiophores were branched, with phialides arranged in a brush-like structure, and conidia were attached in chains at the tip of the phialides. Spores were spherical, small, and unicellular, and 3 µm diameter.</p>
NT9.3		<p><i>Penicillium</i> sp. 2: The colony was round. The colony was round. Initially, the fungal layer was white and smooth, with concentric circles and an ivory-white border, then green-gray. The fungus often grew in clusters on a petri. Phialides overlap each other like a broom. Conidia were small, unicellular, spherical, 3-4 µm diameter, and attached in chains at the tip of the phialides.</p>
T3X		<p><i>Talaromyces</i> sp.: The fungal colonies were round, grey, and multiple layers forming concentric circles. Phialides overlap, resembling the shape of a broom. Conidia were small, unicellular, 3 µm diameter, and were attached in chains at the tip of phialides.</p>
MS5		<p><i>Trichoderma</i> sp. 1: The fungal colonies were spongy and white and turned grey-green when they matured. Fungal hyphae were colorless, multicellular, and 3 µm wide. The phialides were cylindrical, bulging in the middle. Conidia were oval with a size of 3×4 µm.</p>
MS9		<p><i>Aspergillus</i> sp.: Initially, the fungal colonies were white with long hyphae growing on the surface of the medium, forming a velvety layer. Then colony was black in color. At the maturation, sclerotia appeared on the palate. The back of colonies from colorless to pale yellow. The hyphae were branched, multicellular, and 2 µm wide. The hyphae form conidiophore, which attaches to pear-shaped sterigmata measuring 6×1 µm. On the tip of the sterigmata, spherical conidia with a diameter of 3 µm were formed and arranged in chains.</p>
MS4		<p><i>Trichoderma</i> sp. 2: The fungal colonies were spongy, ivory-white in color, and divided into three concentric circles (three layers). The inner and outer circles of the colony were white, while the middle circle was narrower and darker. As the fungus aged, it turned a grayish-green color. The hyphae were colorless and multicellular, with long, branched conidiophores. The phialides were cylindrical and swollen in the middle. The conidia were oval-shaped, 2×3 µm in size.</p>
M26		<p><i>Purpureocillium</i> sp.: The fungal colonies were initially pinkish-white, with a smooth surface forming concentric circles. After five days, the fungal colonies gradually turned purple. The back of the colony was ivory-white, slightly yellow. The phialides were cylindrical in shape, and the conidia were oval, measuring 2×2.5 µm, arranged in chains at the tip of the phialides</p>

X4			<i>Trichoderma</i> sp. 3: The fungus grew well on the PDA medium. Colonies were initially white and interspersed with grey rings that formed concentric rings. Then it turned grey-green color, with a surface covered in a spongy layer. The hyphae were colorless and septate. The phialides are branched in threes. The conidia were oval-shaped, measuring 2.5×4.0 µm.
X0			<i>Trichoderma</i> sp. 4: The fungal colonies were grey-green, with a surface covered in a spongy layer. The hyphae were colorless, multicellular, and 3 µm in width. The conidia were oval-shaped, measuring between 3-4×4-5 µm.
MS43			<i>Chaetomium</i> sp.: The initial color of the colonies was pinkish-white, and the surface layer of the colony was as smooth as velvet. Then it turned red color. The back of the colonies was reddish-purple. The perithecium was oval-shaped, reddish-brown in color, and 140×130 µm in size; there were many curly hairs on the top of the perithecia. Inside the perithecium were ascus-shaped ties; each sac contained eight bean-shaped ascospores 11×8 µm in size.

**Table 2.** Scientific name based on BLAST output and ITS length of 10 fungal samples

Fungal isolates	Accession numbers	Length	Identity	Scientific names	Strain codes
M24	MW113607.1	535 bp	100%	<i>Penicillium janthinellum</i>	Pj-LHOP2
NT9.3	KX766390.1	446 bp	99.78%	<i>Penicillium simplicissimum</i>	Ps-LHOP1
T3X	OM372777.1	490 bp	99.59%	<i>Talaromyces pinophilus</i>	Tp-LHOP1
MS5	KU729029.1	536 bp	100%	<i>Trichoderma virens</i>	Tv-LHOP1
MS9	KY022748.1	538 bp	100%	<i>Aspergillus carbonarius</i>	Ac-LHOP1
MS4	MT176459.1	539 bp	100%	<i>Trichoderma virens</i>	Tv-LHOP2
M26	PP385632.1	535 bp	100%	<i>Purpureocillium lilacinum</i>	Pl-LHOP1
X4	MF992201.1	535 bp	100%	<i>Trichoderma koningiopsis</i>	Tk-LHOP1
X0	MT176459.1	533 bp	100%	<i>Trichoderma virens</i>	Tv-LHOP3
MS43	KF305757.1	523 bp	100%	<i>Chaetomium cupreum</i>	Cc-LHOP1

### Characterization of the decomposition capacity for insoluble phosphate, cellulose, and xylan

#### Phosphate solubilizing test

Many fungal species have the ability to solubilize insoluble phosphate and convert it into an accessible form, known as orthophosphate ions. Plants then absorb these ions, promoting plant growth and agricultural productivity while improving soil health (Kumar et al. 2023). The phosphate-decomposing enzyme activity of ten fungal strains isolated from the rhizosphere of *N. speciosa* is shown in Figure 3. Positive (+) fungal strains in PVK agar medium formed a halo zone around the colony, indicating they can solubilize phosphate in PVK media. In contrast, colonies that did not form halo zones showed negative results. In this study, 5/10 fungal strains produced phosphate decomposing enzyme (+), and 5/10 strains were negative. The positive strains were Tv-LHOP1, Ac-LHOP1, Tv-LHOP2, Tk-LHOP1, and Tv-LHOP3. The 5 negative strains that did not show the ability to degrade insoluble phosphate belonged mainly to *Penicillium* (2 strains), *Talaromyces* (1 strain), *Purpureocillium* (1 strain), and

*Chaetomium* (1 strain).

Results exhibited that the index for phosphate decomposition in five strains ranged from 2.08 to 2.22, indicating their varying efficiencies in converting insoluble phosphate into a form accessible to plants. Notably, Tv-LHOP3 (*Trichoderma virens* LHOP3) and Tk-LHOP1 (*Trichoderma koningiopsis* LHOP1) exhibited the highest phosphate solubilization index, PSI of two strains were 2.22 and 2.18, respectively, followed by Tv-LHOP1 (*Trichoderma virens* LHOP1), Tv-LHOP2 (*Trichoderma virens* LHOP2), and Ac-LHOP1 (*Aspergillus carbonarius* LHOP1), which also showed significant solubilization capabilities but to a lesser extent (Figure 4). Phosphate-solubilizing fungi (PSF) play a crucial role in enhancing the solubilization of insoluble phosphate compounds in soils. The finding of the present study showed that five fungal isolates, namely *Penicillium*, *Talaromyces*, *Chaetomium*, and *Purpureocillium* did not dissolve phosphate, while fungal isolates, such as *Trichoderma* and *Aspergillus* exhibited the capacity to dissolve insoluble phosphate. Doilom et al. (2020) explored phosphate

solubilization of not only *Aspergillus* but also *Penicillium* and *Talaromyces* fungal strain. *Aspergillus hydei* sp. nov. was the most effective strain with the greatest PSI. Elfiati et al. (2021) isolated 12 fungal strains from a peat environment and evaluated their capacity to degrade phosphate. According to their study, the five most effective strains were all *Aspergillus niger*, which showed that all strains could break down phosphate to varied degrees. The findings of the present study were similar to the previous publication on *Trichoderma* strains and *Aspergillus*, which were isolated from soil. Phosphate solubility efficacy is variable and depends on the strain (Xiao et al. 2015; Prasad et al. 2023). The high PSI values of *Tv*-LHOP3 and *Tk*-LHOP1 suggest their strong potential for use in biofertilizer formulations, which could reduce the reliance on chemical fertilizers and support sustainable farming practices (Agnieszka 2018).

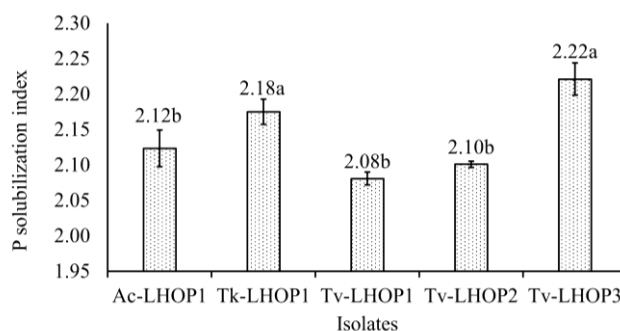


**Figure 4.** P solubilization index of five positive fungal strains in PVK medium after the 5th day of incubation. The expressed values represent the mean of the three replicates. The different letters that follow the top side of the bars showed statistical significance with a value of P value < 0.05

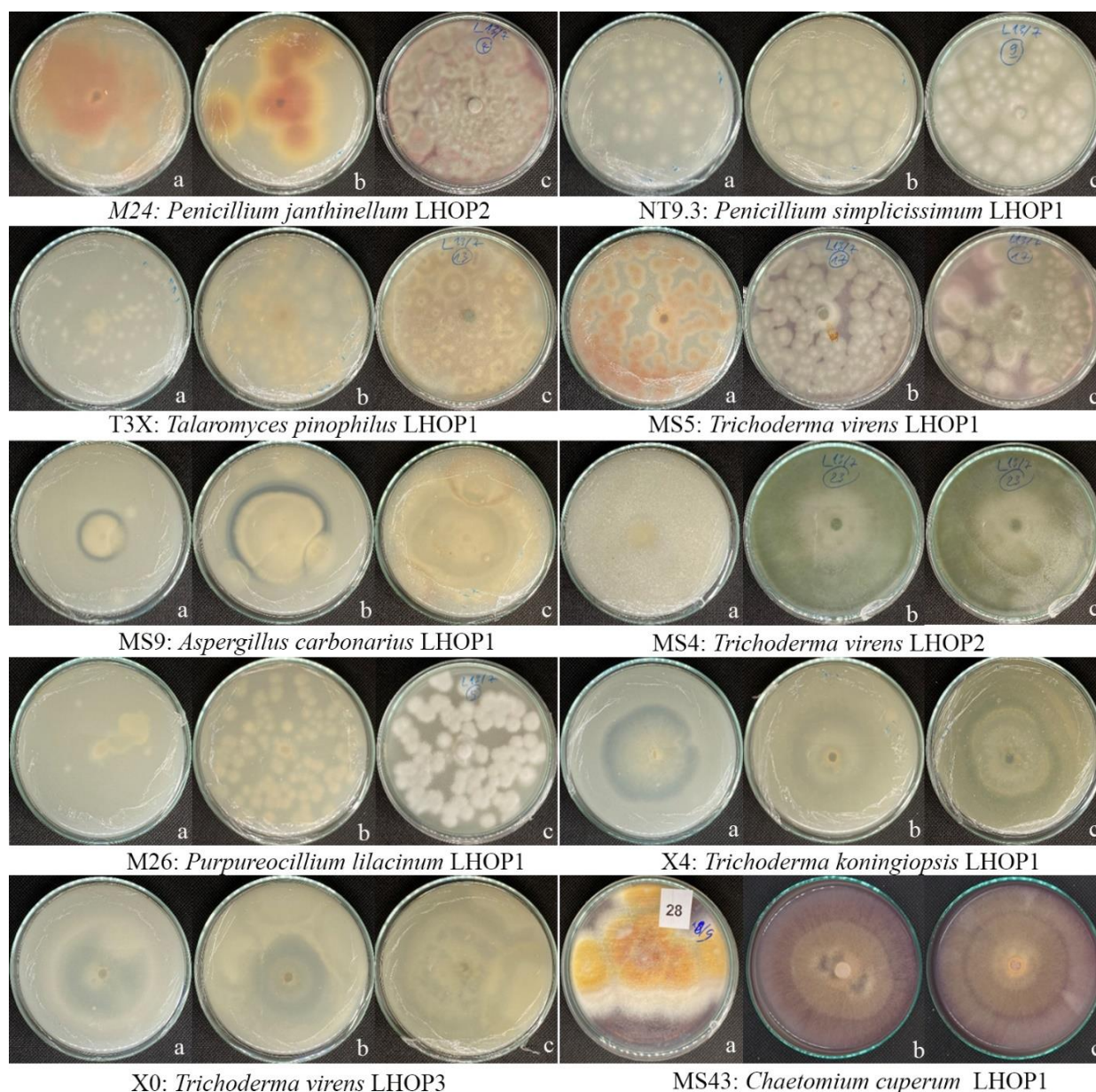


**Figure 3.** Colony and halo zones of fungal isolates for phosphate solubilization on PVK agar (top view). a, b, and c were the halo zones after 1, 3, and 5 days of culture, respectively

### Cellulose decomposition test

In lignocellulosic materials, cellulose makes up the majority of polysaccharides, with a percentage ranging from 40% to 50% (Chaurasia 2019). Several studies have identified fungal strains capable of degrading cellulose in soil. In this study, ten different fungal strains collected from the rhizospheric soil of *N. speciosa* were evaluated for CMC decomposition ability (Figure 5). Among the fungal strains examined, Pj-LHOP2 (*Penicillium janthinellum* LHOP2) demonstrated the highest (7.52 cm) cellulose decomposition capacity, followed by Tk-LVHOP1 (*Trichoderma koningiopsis* LHOP1) with a notable cellulose decomposition value of 7.38 cm (Figure 6). This result is consistent with other research showing that *P. janthinellum* species have a better cellulolysis ability than *Trichoderma* species (Sreeja-Raju et al. 2020). Higher levels of induction, more secreted CAZymes, and a high relative ratio of beta-glucosidase to cellulases are believed to contribute to its ability to break down biomass efficiently (Sreeja-Raju et al. 2020). On the contrary, the cellulose decomposition capacities of Tp-LHOP1 (*Talaromyces pinophilus* LHOP1) and Ac-LHOP1 (*Aspergillus carbonarius* LHOP1) were significantly lower, with cellulose decomposition values of 4.22 cm and 4.88 cm, respectively. The remaining six strains had cellulose decomposition values ranging from 4.65 to 6.75 cm, indicating a modest cellulose breakdown capacity.

### Xylan decomposition assay

Xylans, a polysaccharide with  $\beta$ -1,4 connected D-xylose units, constitute the majority of hemicelluloses in hardwoods, accounting for 15% to 30% of their dry weight (Chaurasia 2019). The isolates were evaluated for their ability to decompose hemicellulose, and the results were quantified in terms of the clearance zone diameter observed on agar plates (Figure 7).

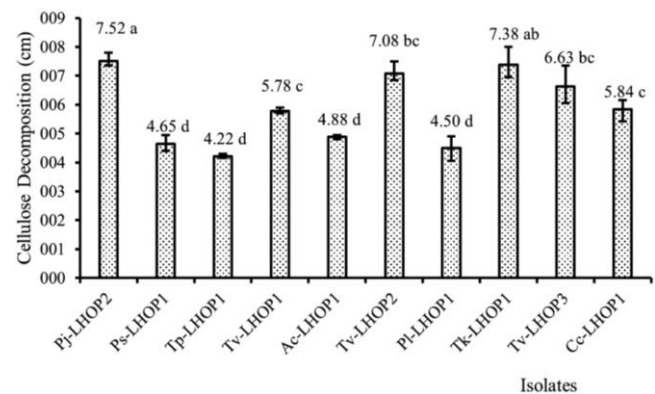


**Figure 6.** The cellulose decomposition ability of 10 fungal strains collected from the soil. The different letters that follow the top side of the bars showed statistical significance with a value of P value < 0.05

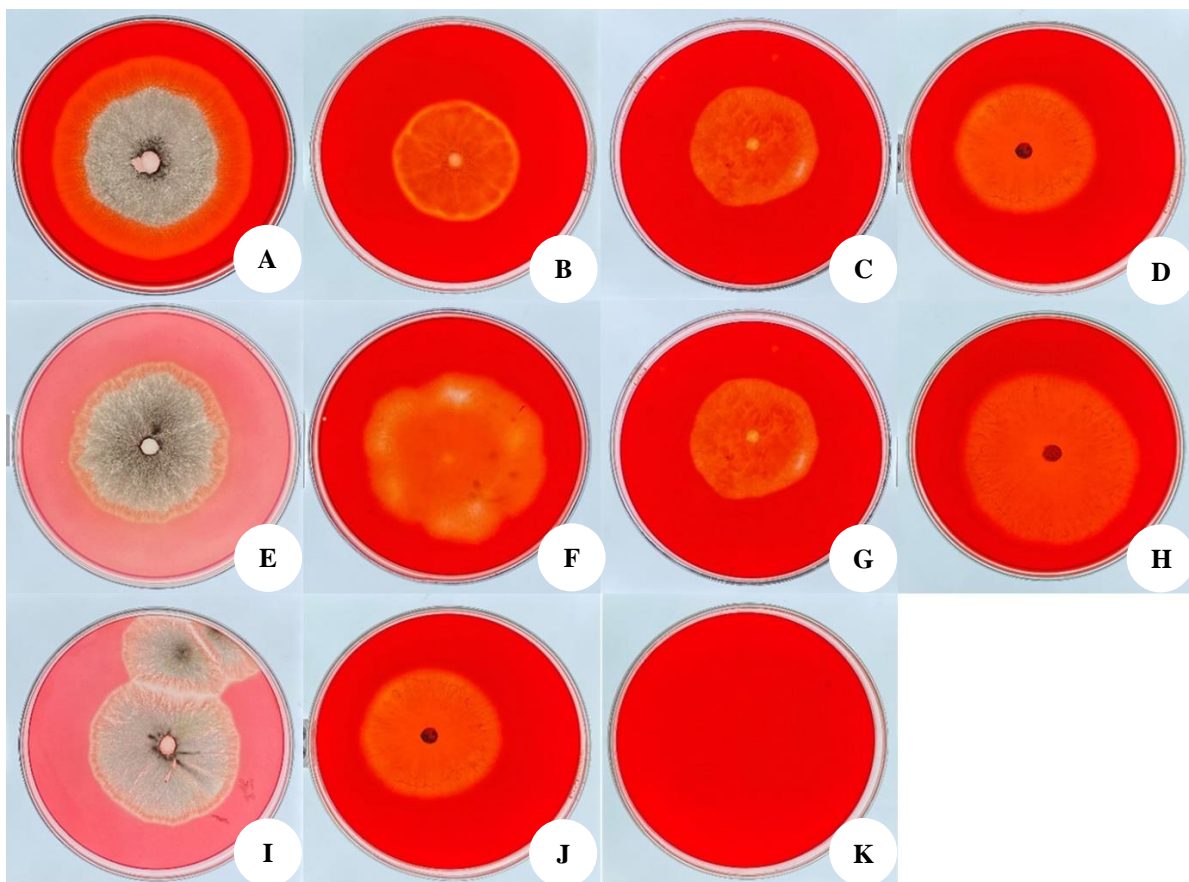


**Figure 5.** Colony and halo zones of fungal isolates collected from the soil on PDA contained Red Congo. A. Pj-LHOP2; B. Ps-LHOP1; C. Tp-LHOP1; D. Tv-LHOP1; E. Ac-LHOP1; F. Tv-LHOP2; G. Pl-LHOP1; H. Tk-LHOP1; I. Tv-LHOP3; J. Cc-LHOP1; K. The control

The results demonstrated that Tv-LHOP2 (*Trichoderma virens* LHOP2) had the highest xylan decomposition with a halo diameter of 8.87 cm, indicating strong hemicellulose decomposition ability (Figure 8). Following, Tk-LHOP1 (*Trichoderma koningiopsis* LHOP1) and Tv-LHOP3 (*Trichoderma virens* LHOP3) were strains that they lower exhibited with halo diameter of xylan decomposition of 8.80 cm and 8.63 cm, respectively. This underscores the potential of this strain to play a significant role in the hemicellulose degradation process (Christopher et al. 2023). On the contrary, the remaining isolates demonstrated moderate to low hemicellulose decomposition abilities, with Tp-LHOP1 (*Talaromyces pinophilus* LHOP1) and Tv-LHOP1 (*Trichoderma virens* LHOP1) recording the lowest xylan decomposition at 2.15 cm and 2.27 cm, respectively (Figure 8). The exceptional performance of Tv-LHOP2, Tk-LHOP1, and Tv-LHOP3 suggests the presence of potentially unique enzymatic activities or genetic factors that facilitate hemicellulose breakdown. The results of the present study were consistent with the finding that the genera *Penicillium*, *Aspergillus*, and *Trichoderma* are good producers of xylan degradation. *Trichoderma reesei*, for example, has been used to create xylanase on an industrial scale, and species of *Aspergillus* and *Penicillium* can produce a variety of xylanase isoforms, some of which are classified as thermophilic xylanases (Bhardwaj et al. 2019; Méndez-Líte et al. 2021).

Local beneficial microorganisms are used for biofertilizer production, which plays a vital role in promoting sustainable agriculture and effective soil management practices via enhancing soil fertility, plant growth, and crop productivity (Fasusi et al. 2021), making nutrients available

to plants and reducing the need for chemical fertilizers (Alori et al. 2017). They also improve plant tolerance to abiotic and biotic stresses, manage phytopathogens, and produce volatile organic compounds beneficial to plants (Fasusi et al. 2021). The production of solid-based or liquid biofertilizers involves several key steps, including the preparation of inoculum, the addition of cell protectants like glycerol, lactose, and starch, selecting an appropriate carrier material, ensuring proper packaging, and determining the most effective delivery methods (Kumar et al. 2021).

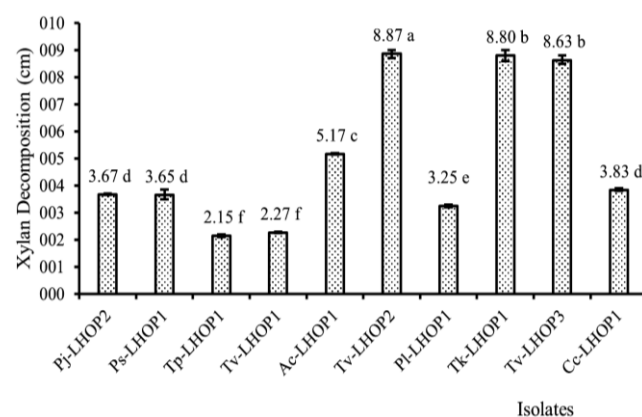


**Figure 8.** The xylan decomposition ability of 10 fungal strains collected from the soil. The different letters that follow the top side of the bars showed statistical significance with a value of P value < 0.05

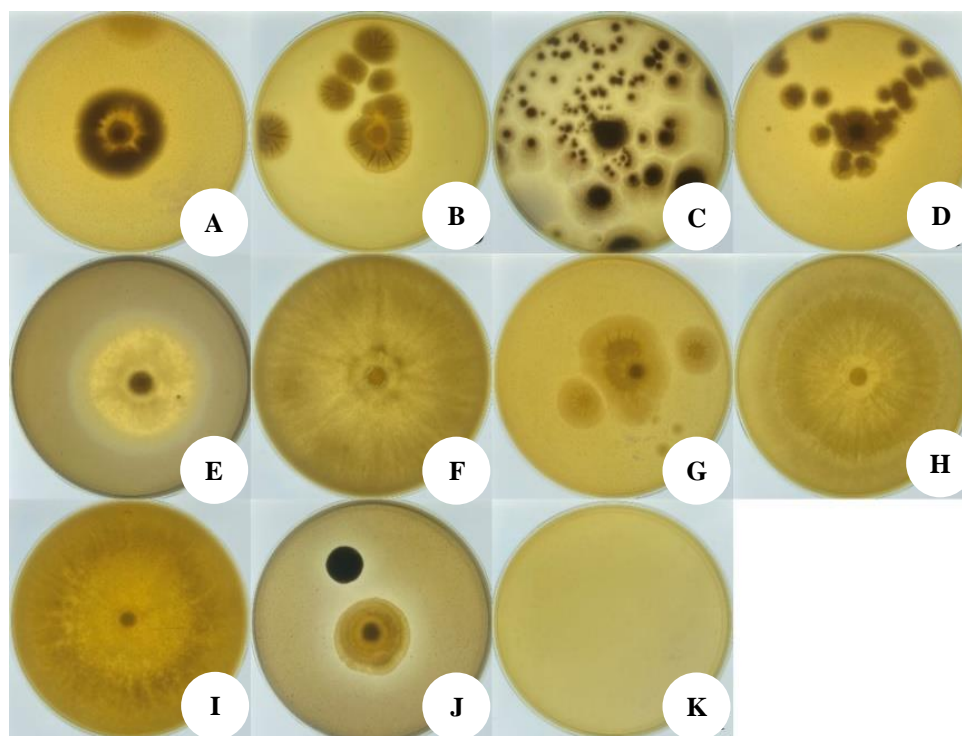


**Figure 7.** Colony and halo zones of fungal isolates collected from the soil. A. Pj-LHOP2; B. Ps-LHOP1; C. Tp-LHOP1; D. Tv-LHOP1; E. Ac-LHOP1; F. Tv-LHOP2; G. Pl-LHOP1; H. Tk-LHOP1; I. Tv-LHOP3; J. Cc-LHOP1; K. The control

Moreover, the biofertilizer efficacy on the growth, development, and yield of the plant was investigated, particularly affected by these abiotic environmental factors, including soil pH, temperature, precipitation, and climate conditions (Bahram et al. 2018). Recent advancements in formulation techniques also include methods such as entrapment or microencapsulation, nano-immobilization of microbial bioinoculants, and the development of biofilm-based biofertilizers (Kumar et al. 2021).

In conclusion, 72 fungal isolates were obtained from the soil of the *N. speciosa* rhizosphere across different regions of northern Vietnam. These isolates primarily belonged to six genera: *Penicillium*, *Trichoderma*, *Aspergillus*, *Talaromyces*, *Purpureocillium*, and *Chaetomium*. Notably, *Penicillium* had the highest number of strains, accounting for more than 50% of isolates in all three studied areas. Molecular analysis using ITS sequences confirmed the morphological identification. Further investigation focused on 10 selected fungal strains (5 from Bac Giang, 3 from Lang Son, and 2 from Vinh Phuc). Among these strains, only five exhibited phosphate-decomposing enzyme activity. Tv-LHOP3 (*Trichoderma virens* LHOP3) and Tk-LHOP1 (*Trichoderma koningiopsis* LHOP1) demonstrated the highest phosphate solubility. Additionally, all strains expressed cellulose and xylan degradation capabilities. In particular, Pj-LHOP2 (*Penicillium janthinellum* LHOP2) demonstrated an impressive efficiency in cellulose degradation, with a halo diameter of 7.52 cm, closely followed by Tk-LVHOP1 (*Trichoderma koningiopsis* LHOP1) with a halo diameter of 7.38 cm. For xylan degradation, Tv-LHOP2 (*Trichoderma virens* LHOP2) exhibited the highest activity (the halo diameter of 8.87 cm). These findings highlight the potential of these fungi as biofertilizers, contributing to nutrient cycling and enhancing sustainable agricultural practices. To apply potential fungal strains to promote sustainable agricultural practices in diverse and complex soil ecosystems, further study should focus on the interaction of various fungal strains- medicinal plants, environmental conditions, field trials of microbial consortia, and long-term studies.

## ACKNOWLEDGEMENTS

This work was supported by the Vietnam Ministry of Education and Training for the Research Project (Project No: B.2023-SP2-02).

## REFERENCES

- Agnieszka S. 2018. Phosphorus microbial solubilization as a key for phosphorus recycling in agriculture. In: Tao Z (eds). Phosphorus-Recovery and Recycling. IntechOpen, Croatia. DOI: 10.5772/intechopen.74920.
- Alori ET, Glick BR, Babalola OO. 2017. Microbial phosphorus solubilization and its potential for use in sustainable agriculture. *Front Microbiol* 8: 971. DOI: 10.3389/fmicb.2017.00971.
- Bahram M, Hildebrand F, Forslund SK et al. 2018. Structure and function of the global topsoil microbiome. *Nature* 560 (7717): 233-237. DOI: 10.1038/s41586-018-0386-6.
- Bala K. 2022. Microbial fertilizer as an alternative to chemical fertilizer in modern agriculture. In: Prasad R, Zhang SH (eds). Beneficial microorganisms in agriculture. Springer, Singapore. DOI: 10.1007/978-981-19-0733-3\_4.
- Bedaawy MY, Awadalla OA, Metwally MA, Samad A. 2022. Isolation, identification, and detection of ligninolytic capability of some fungi isolated from soil samples in Egypt. *Egypt J Exp Biol (Bot)* 18 (1): 197-204. DOI: 10.5455/egyjebb.20220629084930.
- Bhardwaj N, Kumar B, Verma P. 2019. A detailed overview of xylanases: An emerging biomolecule for current and future prospective. *Bioresour Bioprocess* 6 (1): 40. DOI: 10.1186/s40643-019-0276-2.
- Bhattacharyya C, Roy R, Tribedi P, Ghosh A, Ghosh A. 2020. Biofertilizers as substitute to commercial agrochemicals. In: Prasad MNV (eds). Agrochemicals detection, treatment and remediation. Butterworth, Heinemann. DOI: 10.1016/B978-0-08-103017-2.00011-8.
- Chauiyakh O, El Fahime E, Ninich O, Aarabi S, Bouziani M, Chaouch A, Et tahir A. 2023. Short notes: First report of the lignivorous fungus *Paecilomyces maximus* in *Cedrus atlantica* M. in Morocco. *J Wood Sci* 68 (2): 403-412. DOI: 10.37763/wr.1336-4561/68.2.403412.
- Chaurasia B. 2019. Biological pretreatment of lignocellulosic biomass (Water hyacinth) with different fungus for enzymatic hydrolysis and bio-ethanol production resource: Advantages, future work and prospects. *Acta Sci Agric* 5 (3): 89-96. DOI: 10.1016/B978-0-12-815162-4.00007-0.
- Christopher M, Sreeja-Raju A, Kooloth-Valappil P, Gokhale DV, Sukumaran RK. 2023. Correction to: Cellulase hyper-producing fungus *Penicillium janthinellum* NCIM 1366 elaborates a wider array of proteins involved in transport and secretion, potentially enabling a diverse substrate range. *Bioenergy Res* 16 (1): 74. DOI: 10.1007/s12155-022-10476-4.
- Doilom M, Guo JW, Phookamsak R, Mortimer PE, Karunarathna SC, Dong W, Liao CF, Yan K, Pem D, Suwannarach N, Promputtha I, Lumyong S, and Xu JC. 2020. Screening of phosphate-solubilizing fungi from air and soil in Yunnan, China: Four novel species in *Aspergillus*, *Gongronella*, *Penicillium*, and *Talaromyces*. *Front Microbiol* 11: 585215. DOI: 10.3389/fmicb.2020.585215.
- Elfiati D, Delvian D, Hanum H, Susilowati A, Rachmat HH. 2021. Potential of phosphate solubilizing fungi isolated from peat soils as inoculant biofertilizer. *Biodiversitas* 22 (6): 3042-3048. DOI: 10.13057/biodiv/d220605.
- Elfiati D, Susilowati A, Modes C, Rachmat HH. 2019. Morphological and molecular identification of cellulolytic fungi associated with local raru species. *Biodiversitas* 20: 2348-2354. DOI: 10.13057/biodiv/d200833.
- Fasusi OA, Cruz C, Babalola OO. 2021. Agricultural sustainability: Microbial biofertilizers in rhizosphere management. *Agriculture* 11 (2): 163. DOI: 10.3390/agriculture11020163.
- Han LR, Zhang SX, Zhu CS, Zhang X. 2008. Screening and identification of superior fungus degraded cellulose. *J Northwest Agric For Univ* 36 (9): 169-174. [Chinese]
- Huang Z, Zeng YJ, Chen X, Luo SY, Pu L, Li FZ, Zong MH, Lou WY. 2020. A novel polysaccharide from the roots of *Milletia speciosa* Champ: Preparation, structural characterization and immunomodulatory activity. *Intl J Biol Macromol* 145: 547-557. DOI: 10.1016/j.ijbiomac.2019.12.166.
- Kumar M, Shankar A, Chaudhary S, Prasad V. 2023. Phosphate solubilizing microorganisms: Multifarious applications. In: Chhabra S, Prasad R, Maddela NR, Tuteja N (eds). In: Plant Microbiome for Plant Productivity and Sustainable Agriculture 37: 245-262. Springer Nature, Singapore. DOI: 10.1007/978-981-19-5029-2\_10.
- Kumar S, Diksha, Sindhu SS, Kumar R. 2021. Biofertilizers: An ecofriendly technology for nutrient recycling and environmental sustainability. *Curr Res Microb Sci* 3: 100094. DOI: 10.1016/j.crmicr.2021.100094.
- Li J, Sun X, Li M, Zou J, Bian H. 2022. Effects of stand age and soil organic matter quality on soil bacterial and fungal community composition in *Larix gmelinii* plantations, Northeast China. *Land Degrad Dev* 33 (8): 1249-1259. DOI: 10.1002/ldr.4219.
- Liu JM, Xiong X, Li, Liu, Li LX, Luo C. 2017. Fungal diversity in the rhizosphere soil of *Drepanostachyum luodianense*. *Mycosystema* 36 (2): 260-266. DOI: 10.13346/j.mycosystema.160024.
- M'barek HN, Taidi B, Smaoui T, Aziz MB, Mansouri AM, Hajjaj H. 2019. Isolation, screening and identification of ligno-cellulolytic fungi from northern central Morocco. *Biotechnol Agron Soc Environ* 23 (4): 207-217. DOI: 10.25518/1780-4507.18182.
- Méndez-Lítez JA, de Eugenio LI, Nieto-Domínguez M, Prieto A, Martínez MJ. 2021. Hemicellulases from *Penicillium* and *Talaromyces* for lignocellulosic biomass valorization: A review. *J Bioresour Technol* 324: 124623. DOI: 10.1016/j.biortech.2020.124623.

- Nafaa M, Rizk SM, Aly TAGA, Rashed MAS, Abd El-Moneim D, Bacha AB, Alonazi M, Magdy, M. 2023. Screening and identification of the rhizosphere fungal communities associated with land reclamation in Egypt. *Agriculture* 13 (1): 215. DOI: 10.3390/agriculture13010215.
- Pointing S. 1999. Qualitative methods for the determination of lignocellulolytic enzyme production by tropical fungi. *Fungal Divers* 2: 17-33.
- Prasad A, Dixit M, Meena SK, Suman, Kumar A. 2023. Qualitative and quantitative estimation for phosphate solubilizing ability of *Trichoderma* isolates: A natural soil health enhancer. *Materials Today Proc* 81: 360-366. DOI: 10.1016/j.matpr.2021.03.305.
- Raja HA, Miller AN, Pearce CJ, Oberlies NH. 2017. Fungal identification using molecular tools: A primer for the natural products research community. *J Nat Prod* 80: 756-770. DOI: 10.1021/acs.jnatprod.6b01085.
- Rilling JJ, Acuña JJ, Nannipieri P, Cassan F, Maruyama F, Jorquera MA. 2019. Current opinion and perspectives on the methods for tracking and monitoring plant growth-promoting bacteria. *Soil Biol Biochem* 130: 205-219. DOI: 10.1016/j.soilbio.2018.12.012.
- Rogers SO, Bendich AJ. 1989. Extraction of DNA from plant tissues. In: Gelvin SB, Schilperoort RA, Verma DPS (eds). *Plant Molecular Biology Manual*. Springer Netherlands, Dordrecht. DOI: 10.1007/978-94-009-0951-9\_6.
- Sane SA, Mehta SK. 2015. Isolation and evaluation of rock phosphate solubilizing fungi as potential biofertilizer. *J Fert Pes* 06: 156. DOI: 10.4172/2471-2728.1000156.
- Sreeja-Raju A, Christopher M, Kooloth-Valappil P, Kuni-Parambil R, Gokhale, DV, Sankar M, Abraham A, Pandey A, Sukumaran, RK. 2020. *Penicillium janthinellum* NCIM1366 shows improved biomass hydrolysis and a larger number of CAZymes with higher induction levels over *Trichoderma reesei* RUT-C30. *Biotechnol Biofuels* 13 (1): 196. DOI: 10.1186/s13068-020-01830-9.
- Tamura K, Stecher G, Kumar S. 2021. MEGA11: Molecular Evolutionary Genetics Analysis Version 11. *Mol Biol Evol* 38 (7): 3022-3027. DOI: 10.1093/molbev/msab120.
- Tolan JS, Foody B. 1999. Cellulase from submerged fermentation. In: Tsao GT, Brainard, AP, Bungay HR et al. (eds). *Recent progress in bioconversion of lignocellulosics*. Springer Berlin Heidelberg, Berlin, Heidelberg. DOI: 10.1007/3-540-49194-5\_3.
- Wakelin S, Gupta VV, Harvey P, Ryder M. 2007. The effect of *Penicillium* fungi on plant growth and phosphorus mobilization in neutral to alkaline soils from southern Australia. *Can J Microbiol* 53 (1): 106-115. DOI: 10.1139/w06-109.
- White T, Bruns T, Lee S, Taylor J. 1990. Amplification and direct sequencing of fungal ribosomal RNA genes for phylogenetics. In: Innis MA, Gelfand DH, Sninsky JJ, White TJ (eds). *PCR Protocols: A Guide to Methods and Applications*. Academic Press, New York. DOI: 10.1016/B978-0-12-372180-8.50042-1.
- Xiao C, Fang Y, Chi R. 2015. Phosphate solubilization *in vitro* by isolated *Aspergillus niger* and *Aspergillus carbonarius*. *Rev Chem Intermed* 41 (5): 2867-2878. DOI: 10.1007/s11164-013-1395-6.
- Yao S, Lan Z, Huang R, Tan Y, Huang D, Gu J, Pan C. 2021. Hormonal and transcriptional analyses provides new insights into the molecular mechanisms underlying root thickening and isoflavonoid biosynthesis in *Callerya speciosa* (Champ. ex Benth.). *Schot Sci Rep* 11 (1): 9. DOI: 10.1038/s41598-020-76633-x.
- Yu D, Liang X. 2019. Characterization and identification of isoflavonoids in the roots of *Milletia speciosa* Champ. by UPLC-Q-TOF-MS/MS. *Curr Pharm Anal* 15 (6): 580-591. DOI: 10.2174/1573412914666180608095922.
- Zhang Y, Chen FS, Wu XQ, Luan FG, Zhang LP, Fang XM, Wan SZ, Hu XF, Ye JR. 2018. Isolation and characterization of two phosphate-solubilizing fungi from rhizosphere soil of moso bamboo and their functional capacities when exposed to different phosphorus sources and pH environments. *PLoS One* 13 (7): e0199625. DOI: 10.1371/journal.pone.0199625.
- Zhao W, Wang DD, Huang KC, Liu S, Reyila M, Sun YF, Li JN, Cui BK. 2023. Seasonal variation in the soil fungal community structure of *Larix gmelinii* forests in Northeast China. *Front Microbiol* 14: 1106888. DOI: 10.3389/fmicb.2023.1106888.